J. Cent. South Univ. (2015) 22: 377−385
DOI: 10.1007/s11771-015-2532-8

Springer

A comprehensive comparison on vibration and heat transfer of two elastic heat transfer tube bundles

YAN Ke(闫柯)[1], GE Pei-qi(葛培琪)[2], ZHAI Qiang(翟强)[1]

1. Key Laboratory of Education Ministry for Modern Design and Rotor-Bearing System (Xi'an Jiaotong University), Xi'an 710049, China;
2. School of Mechanical Engineering, Shandong University, Jinan 250061, China

Abstract: Elastic heat transfer tube bundles are widely used in the field of flow-induced vibration heat transfer enhancement. Two types of mainly used tube bundles, the planar elastic tube bundle and the conical spiral tube bundle were comprehensively compared in the condition of the same shell side diameter. The natural mode characteristics, the effect of fluid−structure interaction, the stress distribution, the comprehensive heat transfer performance and the secondary fluid flow of the two elastic tube bundles were all concluded and compared. The results show that the natural frequency and the critical velocity of vibration buckling of the planar elastic tube bundle are larger than those of the conical spiral tube bundle, while the stress distribution and the comprehensive heat transfer performance of the conical spiral tube bundle are relatively better.

Key words: planar elastic tube bundle; conical spiral tube bundle; mode characteristics; heat transfer performance

1 Introduction

It has been long recognized that flow-induced vibration can damage the heat transfer device and tubes, especially in shell-and-tube heat exchanger. Much effort has been devoted to the research of the mechanism and influence of flow-induced vibration, both in shell-side fluid flow and tube-side fluid flow, such as the work by WEAVER and FITZPATRICK [1] about single phase flow, and that by PETTIGREW and TAYLOR [2] about two-phase flow. Most of the foregoing studies were concerned on preventing the flow-induced vibration in heat exchangers. However, the essence of vibration is that the mechanical energy continuously accumulates and dissipates [3]. It is almost impossible to completely avoid the vibration of the heat transfer devices. Though the analysis of flow-induced vibration has persisted a long period, the design method for appropriately addressing flow-induced vibration problems in heat exchangers has not been well developed yet.

The technology of heat transfer enhancement via the flow-induced vibration was proposed by CHENG et al [3−4], which was proved as an effective and novel approach in heat transfer enhancement. The main idea of flow-induced vibration in heat transfer enhancement was using elastic tube bundles instead of the traditional rigid tubes. Heat transfer was enhanced via the vibration of the elastic tube bundle which was induced by the fluid flow around it. The elastic tube bundle, driven by the fluid flow around it, vibrated with low frequency and small amplitude around its equilibrium position. The convective heat transfer coefficient increased significantly for low velocity cases. Furthermore, the fouling problem on the heat transfer surface can be related to the flow-induced vibration, namely, the vibration of tube bundles can be employed to restrain the fouling, thus an novel approach of composite heat transfer enhancement was established.

The first elastic tube bundle used in this field was the planar elastic tube bundle, which consisted of four curved pipes and was fixed as a cantilever beam in heat exchangers. Many investigations and improvements about the performance and structure were conducted, such as works by JIANG [5] and SONG et al [6]. Based on the structural constrains of the planar elastic tube bundle, a newly dimensional elastic tube bundle was designed, the conical spiral tube bundle proposed by YAN et al [7]. The mode characteristic, the heat transfer performance and the stress intensity of the two elastic tube bundles were analyzed and discussed.

The present research on the planar elastic tube

Foundation item: Projects(xjj2013104, 08143063) supported by the Fundamental Research Funds for the Central Universities, China; Project(2011CB706606) supported by the National Basic Research Program of China
Received date: 2013−09−18; **Accepted date:** 2014−04−01
Corresponding author: GE Pei-qi; E-mail: pqge@sdu.edu.cn

bundle and the conical spiral tube bundle are independent on a certain extent. A direct comparison of the two types of elastic tube bundle on the mode characteristic, the stress distribution and the heat transfer performance was difficult, because the structural parameters of the two tube bundles in the foregoing research were non-uniform. To this end, the two elastic tube bundles were compared in this work in condition of the same shell side diameter, and a comprehensive comparison of the two tube bundles on the natural vibration characteristic was conducted. The effect of fluid−structure interaction, the stress distribution and the heat transfer performance were studied.

2 Structural parameters

The structure of planar elastic tube bundle is shown in Fig. 1(a), which consists of four curved pipes connected, with two rigid bodies. The ends I and II are fixed, and the ends III and IV are free. In working condition, the inlet of hot medium is at the fixed end I, and the outlet is at the fixed end II. Adjacent planar elastic tube bundles are parallel mounted. Figure 1(b) shows the conical spiral tube bundle, which consists of two helical pipes connected with a rigid body. The ends I and II are fixed, and the end III is free. Adjacent conical spiral tube bundles are nesting mounted in the shell side of heat exchangers.

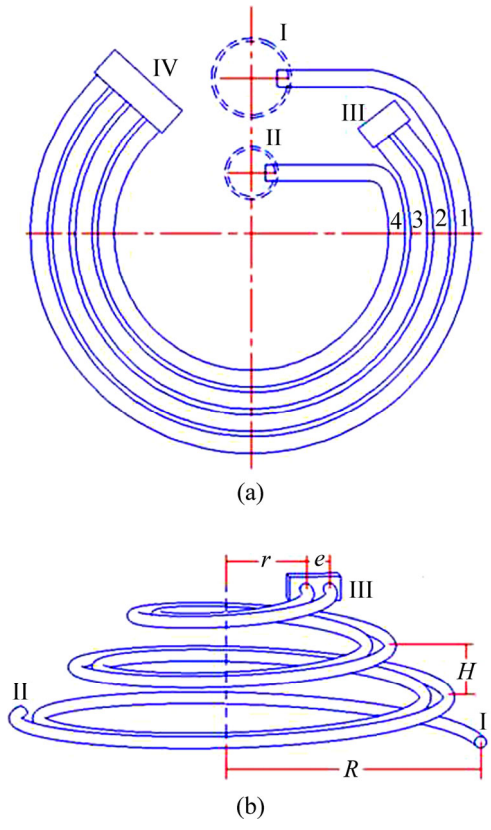

Fig. 1 Structures of two elastic tube bundles: (a) Planar elastic tube bundle; (b) Conical spiral tube bundle

For a direct comparison of the two elastic tube bundles, the models in this work are set up in condition of the same shell-side diameter. The structural parameters of the two tube bundles are given in Table 1.

Table 1 Structural parameter of two elastic tube bundles

Type	Parameter	Value
Planar elastic tube bundle	Shell side diameter/mm	800
	Cross section diameter/mm	20
	Pipe thickness/mm	1.5
	The 1st pipe radius/mm	300
	The 2nd pipe radius/mm	270
	The 3rd pipe radius/mm	240
	The 4th pipe radius/mm	210
	Rigid body size/mm	126×42×30
	Rigid body size/mm	66×42×30
Conical spiral tube bundle	Shell side diameter/mm	800
	Cross section diameter/mm	20
	Pipe thickness/mm	1.5
	Pipe space/mm	30
	Bottom radius/mm	280
	Top radius/mm	80
	Helical pitch/mm	90
	Rigid body size/mm	66×42×30

3 Mode analysis

3.1 Natural mode characteristics

An experiment was conducted to test the natural vibration of the two tube bundles via the hammering method, as seen in Fig. 2 [8−9]. The material of the two tubes is red copper. The inlet and outlet of the tube bundle were totally clamped supported with substructure, which is in large size and weight to minimize the interference in the testing. The testing points were uniformly distributed on the tube bundle. The accelerometer was fixed on the free end IV of planar elastic tube bundle, and on the free end III of the conical spiral tube. The response signal was selected through a charge amplifier and the force sensor was connected with the exciting hammer. The hammerhead used in the experimental is plastic due to the narrow range of tube frequency we cared. A force hammer was used to impulse the testing points, and the response signals were selected by the DASP-V10 data acquisition system.

The finite element method was employed to study the natural mode characteristic of the two elastic tube bundles [7, 10]. Firstly, the elastic tube bundles were divided into many small elements, and the element matrixes, such as the mass matrix and the stiffness

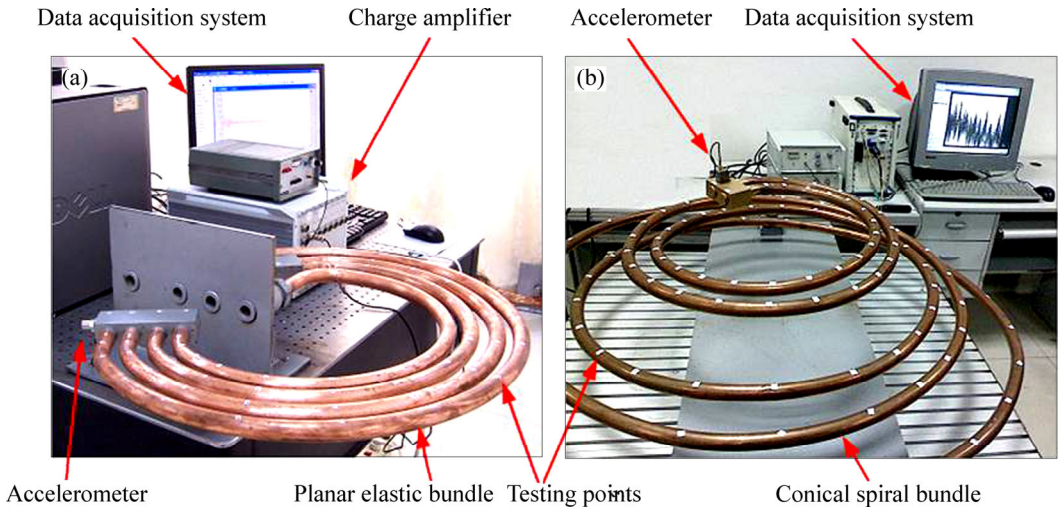

Fig. 2 Mode test of two elastic tube bundles: (a) Planar elastic tube bundle; (b) Conical spiral tube bundle

matrix, were obtained from the Hamilton variational equation [11−13]. Subsequently, the general matrixes of elastic tube bundles were founded and the vibration equations of the tube bundles were obtained.

The vibration equation of the elastic tube bundle is

$$\boldsymbol{M}\ddot{q} + \boldsymbol{K}_{\mathrm{p}} q = 0 \tag{1}$$

where $\boldsymbol{M}$ is the general mass matrix of the tube bundle, $\boldsymbol{K}_{\mathrm{p}}$ is the stiffness matrix, and q is the nodes displacement. The eigenvalue of the vibration matrix can be obtained from Eq. (1) with the mode decomposition method, and the natural frequencies of the elastic tube bundles can be obtained.

A comparison on the experimental data and the calculated result showed that the tolerances on the natural frequencies of the two elastic tube bundles were less than 7% [7] and 8.07% [10], respectively. The natural frequencies of the two tube bundles are shown in Fig. 3. It can be derived that in the similar structural parameters, the lower order frequencies of the planar elastic tube bundle are much larger than those of the conical spiral tube bundle.

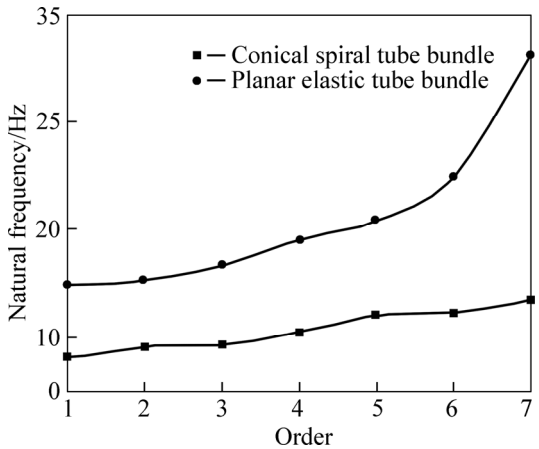

Fig. 3 Natural frequencies of two elastic tube bundles

A further study on the lower order mode shape of the two elastic tube bundles shows that, the natural mode shape of the planar elastic tube bundle includes the in-plane vibration mode and out-plane vibration mode, as seen in Fig. 4. The odd orders of planar elastic tube are in out-plane vibration, while the even orders are in in-plane vibration mode. The natural mode shape of the conical spiral tube bundle is mainly in longitudinal vibration mode, except the 2nd and the 3rd mode shape, which are in transverse vibration mode, as seen in Fig. 5.

3.2 Tube-side FSI

Based on the equation of the natural vibration of the two elastic tube bundles, the effect of tube-side fluid−structure interaction (FSI) of the elastic tube bundles can be solved with the combination of Hamilton variational equation [7, 10] and finite element method. The vibration

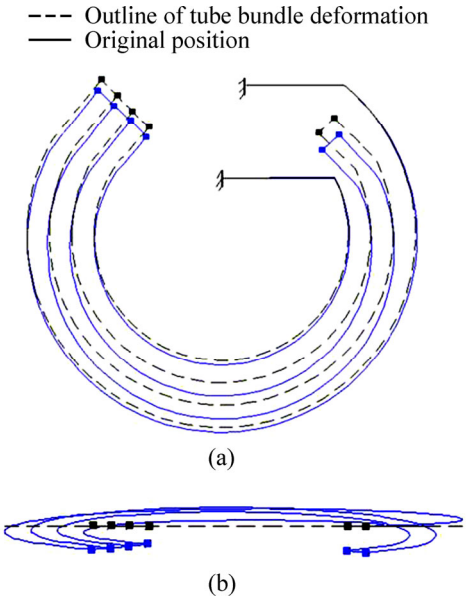

Fig. 4 Mode shape of planar elastic tube bundle: (a) In-plane vibration mode; (b) Out-plane vibration mode

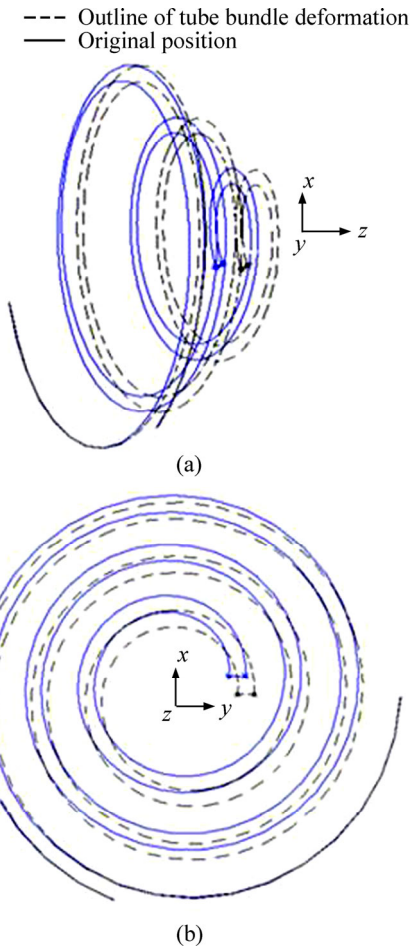

Fig. 5 Natural mode shape of conical spiral tube bundle: (a) Longitudinal vibration mode; (b) Transverse vibration mode

equation of tube bundles in condition of inside fluid flow is

$$\boldsymbol{M}\ddot{q}+c\boldsymbol{G}\dot{q}+\left(\boldsymbol{K}_{\mathrm{p}}-c^{2}\boldsymbol{K}_{\mathrm{f}}\right)q=0 \tag{2}$$

where $\boldsymbol{M}$ is the general mass matrix, c is the flow velocity inside the tube bundle, $\boldsymbol{G}$ is the damp matrix induced by Coriolis force, $\boldsymbol{K}_{\mathrm{p}}$ is the pipe stiffness matrix, and $\boldsymbol{K}_{\mathrm{f}}$ is the fluid kinetic matrix.

In condition of fluid flow inside the tube bundles, the vibration equation can not be solved directly with the mode decomposition method just mentioned above, due to the existence of the asymmetric damp matrix $\boldsymbol{G}$ induced by Coriolis force. In Refs. [11, 14], the vibration equation is turned into the standard eigenvalue equation:

$$\boldsymbol{D}\boldsymbol{\varphi}=-\lambda\boldsymbol{\varphi} \tag{3}$$

where λ is eigenvalue, and $\boldsymbol{\varphi}$ is vector of eigenvalue, which is also the displacement vector of the element nodes.

And $\boldsymbol{D}$ is the dynamic matrix of the system:

$$\boldsymbol{D}=\begin{bmatrix} c\boldsymbol{M}^{-1}\boldsymbol{G} & \boldsymbol{M}^{-1}\left(\boldsymbol{K}_{\mathrm{p}}-c^{2}\boldsymbol{K}_{\mathrm{f}}\right) \\ -\boldsymbol{I} & 0 \end{bmatrix}_{12(n-1)\times 12(n-1)} \tag{4}$$

where n is the number of the finite elements of the tube bundles during the FEM calculation. Here, the eigenvalue of the dynamic matrix $\boldsymbol{D}$ is solved and the frequencies of the tube bundle are obtained.

The effect of water flow inside the tube bundle is discussed. The natural frequency variety of tube bundles at different tube-side flow velocities is shown in Fig. 6. It can be deduced that the fluid flow inside the tube has significant influence on tube bundles frequencies, especially on the lower order modes. The natural frequencies of tube bundle decrease when the velocity of inside flow increases.

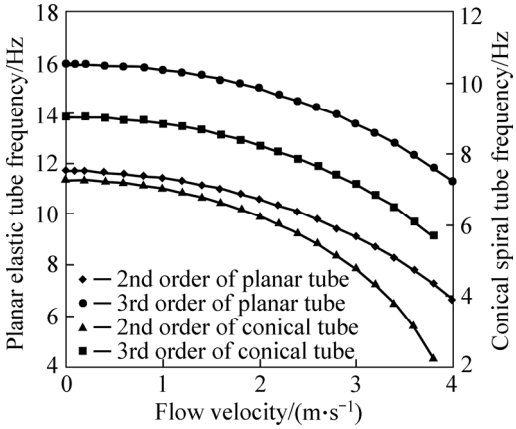

Fig. 6 Effect of tube-side fluid flow on tube natural frequencies

Vibration buckling makes fatal damage to elastic tube bundles in heat exchangers, which induces breakage in tube bundles and hinders the normal circulation in heat exchangers. The vibration buckling of tube bundle happens when the velocity of tube-side flow increases to a critical value, and the first order natural frequency of tube bundle equals zero. The critical velocity of the fluid flow inside the tube bundles is calculated and shown in Fig. 7. It can be seen that the critical velocity of the planar elastic tube bundle is about 3.4 m/s, and the critical velocity of the conical spiral tube bundle is about 1.27 m/s. From Ref. [4], we know that the inside fluid flow speed of elastic tube bundle is between 0.01 m/s

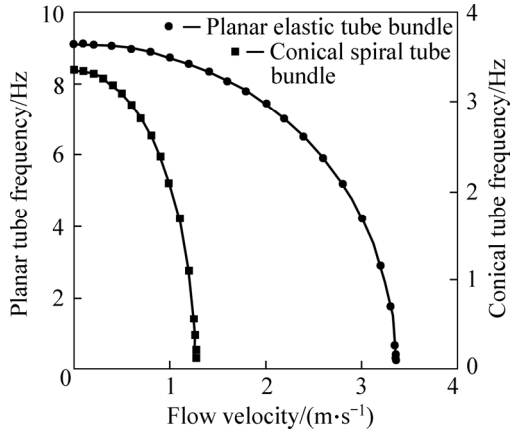

Fig. 7 Critical velocity of two elastic tube bundles

and 0.3 m/s in real working condition, and it is much larger than the critical velocity of the two elastic tube bundles.

3.3 Shell-side FSI

The fluid−structure interaction of the shell-side fluid flow has much significant effect on the vibration of tube bundles, compared with the tube-side fluid flow. The investigation of the vibration characteristic of elastic tube bundles with shell-side fluid flow is highly desirable. Unfortunately, correlative research in this area is rarely developed due to the complex structure of elastic tube bundles in both experiment and numerical simulation. Most of the forgoing researches in this area were focused on the long straight cylinder with circular cross section, such as GUILMINEAU and QUEUTEY [15], GOPALKRISHNAN [16], and SARPKAYA [17].

The resent simulation work on the shell-side fluid flow of planar elastic tube bundle was done by ZHENG [18]. The results show that the shell-side fluid−structure interaction had significant influence on the natural mode characteristics of planar elastic tube bundle. The natural frequencies of planar elastic tube bundle were decreased by about 10% when the shell-side fluid flow speed was equal to zero. The effect of shell-side flow speed on the planar tube bundle was still unclear and research and discussion of this field was highly desirable.

The influence of shell-side fluid flow in the conical spiral tube bundle was mathematically analyzed with finite element method [9], based on the experimental data of GOPALKRISHNAN [16] and the calculation of PAN et al [19]. The calculation was only conducted to the transverse vibration of conical spiral tube bundle, because the fluid force coefficient obtained here was from a cylinder vibrating transversely in the experiment [16]. The transverse vibration frequency of conical spiral tube bundle in shell-side fluid flow was compared with the natural frequency of tube bundle. It is easy to conclude that the effect of shell-side flow on the vibration of tube bundle is significant. The frequency is decreased by about 18%−24% with the outside flow speed U=0.3 m/s.

The comparison of the two elastic tube bundles of the shell-side fluid flow influence is difficult, due to the complex fluid−structure interaction. As mentioned above, the investigation of the vibration characteristic of elastic tube bundles with shell-side fluid flow is highly desirable.

4 Stress analysis

4.1 Maximum stress

The harmonic response method was employed via the FEM software in the stress analysis of the elastic tube bundles. The free end of the two elastic tube bundles were applied with a harmonic force with the same frequency and amplitude. As for the planar elastic tube bundle, the force was applied on the free end IV to make sure the tube bundle vibrating in the out-plane mode shape. As for the conical spiral tube bundle, the force was applied also on the free end III to make sure the tube bundle vibrating in the longitudinal mode shape.

To verify the accuracy of the stress analysis in this work, the maximum stress of the planar elastic tube bundle was calculated theoretically in condition of the same amplitude with the above harmonic analysis. The deflection of the 1st and the 4th pipes (seen in Fig. 1) of the planar elastic tube bundle was obtained with curved deformation energy, based on the stress boundary condition of the curved beam, ignoring the axis displacement and shearing deformation. The detailed derivation can be seen in Ref. [20]. The maximum stress of the fixed end of planar elastic tube bundle in the out-plane vibration can be obtained as

$$\delta_y = \frac{\partial U}{\partial F} = \frac{1}{EI}\int FR^2 \sin^2\theta R\mathrm{d}\theta \tag{5}$$

$$\sigma_{\max} = \frac{M_{\max}}{w_z} + \frac{F}{A} \tag{6}$$

where U is distortion energy, F is symmetrical force on the free ends, R is pipe curving radius, δ_y is deflection of the tube, θ is the cross section rotation angle, $\sigma_{\max}$ is maximum tensile stress, $M_{\max}$ is the moment of the bundles fixed end, w_z is the bending section modulus, and A is area of cross section. A comparison on the maximum stress of planar elastic tube bundle shows that the theoretical value and the simulation data in this work are similar, and the biggest error is less than 7%.

The stress distribution of the two elastic tube bundles is shown in Fig. 8. As for the planar elastic tube bundle, the stress concentrates on the 4th pipe, and the maximum stress ("MX" in Fig. 8) presents at the point where the pipe curvature is the biggest. As for the conical spiral tube bundle, the stress distribution is uniformly increased from the free end to the fixed end, and the maximum stress presents at the fixed end I. The maximum stresses of the two elastic tube bundles are listed in Table 2. It can be derived that the fixed end stress of the conical spiral tube is much smaller than that of the planar elastic tube bundle. The maximum stress of conical spiral tube bundle is about 1/5 compared to that of the planar elastic tube bundle in the same vibration amplitude. The structural support of the planar elastic tube bundle is a quasi-cantilever beam. Therefore, the stress of the fixed end is concentrated. The structural support of the conical spiral tube bundle is a quasi simply supported beam, and the stress distribution is much uniform.

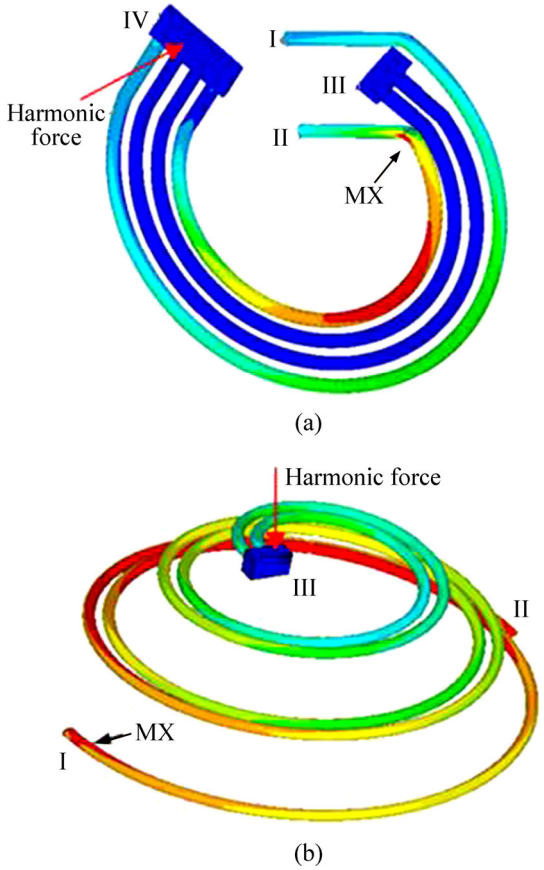

Fig. 8 Stress distribution of two elastic tube bundles: (a) Planar tube bundle; (b) Conical spiral tube bundle

Table 2 Maximum stress of two elastic tube bundles

Amplitude/mm	Maximum stress/MPa	
	Planar elastic tube bundle	Conical spiral tube bundle
9	52.8736	9.9617
28	106.5134	23.7548
47	212.2605	46.7433

4.2 Optimum of tube bundle

As mentioned above, the stress of the planar elastic tube bundle is concentrated, and the maximum stress is 4 times larger than that of the conical spiral tube bundle. So, the optimization of structural design of the planar elastic tube bundle is highly desirable. The optimal structure of planar elastic tube bundle is proposed to improve the mode characteristic, heat transfer area of unit volume, and the stress concentration of the fixed end [5]. The experimental data show that, in the same tube space, the heat transfer area per unit volume is increased by 25%, and the heat transfer coefficient is also increased because of the decline of the tube rigid and the increase of the tube vibration intensity. Above all, the maximum stress of the improved structural on the foxed end is just 1/6 compared to the primary one.

5 Heat transfer performance

5.1 Inner surface heat transfer

Heat transfer performance of the two elastic tube bundles was analyzed with Fluent software. The model of planar elastic tube bundle was set up with the Cartesian coordinate and the conical spiral tube was founded with cylindrical coordinate. The inner surface was divided with the boundary layer technology, and the cross section was meshed with the non-structure grids. During the simulation, the second order upwind algorithm was employed in the discretization of the control equations because of its accuracy and iterating efficiency. The tube inner surface was set to be 308 K, and the fluid flow inside the tube bundle was set to be 298 K.

The heat transfer rate per unit area and the pressure lose per unit length of the two elastic tube bundles are shown in Fig. 9. It can be derived that the heat transfer rate of the conical spiral tube bundle is about 1.5 times that of the planar elastic tube bundle in laminar fluid flow. Meanwhile, the pressure loss of conical spiral tube bundle is somewhat larger than that of the planar elastic tube bundle, as seen in Fig. 9.

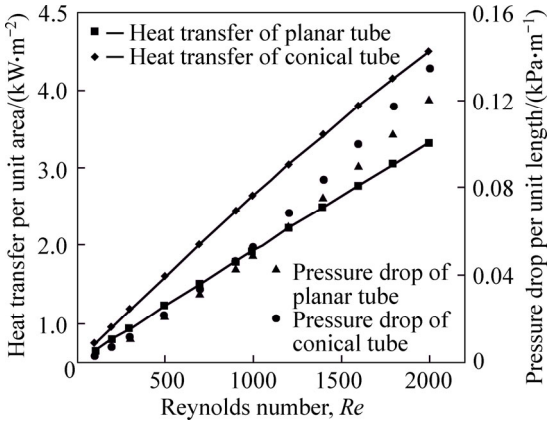

Fig. 9 Heat transfer and pressure drop of two elastic tube bundles

In order to conduct a comprehensive comparison of the heat transfer and pressure drop of the two elastic tube bundles, the performance evaluation criteria (PEC) values of the two tube bundles are denoted as [20]

$$P_1 = (Nu_1 / Nu_0)/(f_1 / f_0)^{1/3} \quad (7)$$

$$P_2 = (Nu_2 / Nu_0)/(f_2 / f_0)^{1/3} \quad (8)$$

where Nu_0 and f_0 respectively denote the heat transfer performance and pressure drop of a bare tube. Nu_1, Nu_2 and f_1, f_2 respectively denote the parameters of the planar elastic tube bundle and the conical spiral tube bundle. It is indicated that the comprehensive performance of conical spiral tube bundle is about 1.5 times that of the

planer elastic tube bundle, in the condition of inside fluid flow.

5.2 Secondary fluid flow

The above research on the heat transfer performance of the two elastic tube bundles indicates that, without taking account of the shell side fluid flow and pipe vibration, the comprehensive performance of conical spiral tube bundle is about 1.5 times that of the planar elastic tube bundle. The reason is that the secondary fluid flow inside the conical spiral tube bundle is much intensive than that inside the planer elastic tube bundle.

The secondary fluid flow inside the tube bundles is also analyzed in this work. The secondary fluid flow on the cross sections of the two tube bundles is shown in Fig. 10, in which the arrow denotes the direction of the centrifugal force. The planar elastic tube bundle is made up of four curved pipes, and the secondary fluid flow of it is similar to the commonly curved tube. Therefore, the secondary fluid flow of planer elastic tube bundle is weak. The structure of conical spiral tube bundle is helically shaped, and the fluid flow inside the tube is affected by the centrifugal force and Coriolis force [21]. The contour of the secondary fluid flow is complicated,

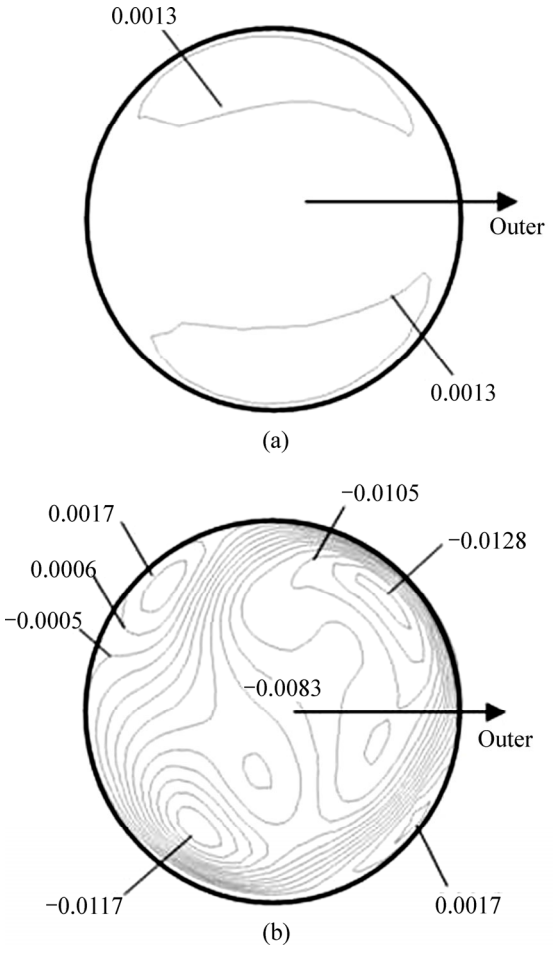

Fig. 10 Secondary fluid flow of two elastic tube bundles: (a) Planar elastic tube bundle; (b) Conical spiral tube bundle

where four independent parts of secondary flow in each cross section exist and the flow directions are different from each other. It can be derived that the secondary fluid flow of conical spiral tube bundle is more intensive than that of the planar elastic tube bundle, and the heat transfer performance of conical spiral tube bundle is better.

A further analysis on the heat transfer of the tube-side fluid flow of conical spiral tube bundle is conducted with the field synergy principle [22−23]. The comprehensive heat transfer of the tube-side fluid flow is evaluated with the synergy angle γ, which is the angle between the temperature gradient vector ∇T and velocity gradient vector ∇u [24]. It can be derived that the increase of γ means the increase of tube PEC value:

$$\gamma = \arccos\frac{\nabla T \cdot \nabla u}{|\nabla T||\nabla u|} \propto P \tag{9}$$

The user defined function (UDF) is employed in calculation of the synergy angle of elastic tube bundles. A section along the tube in the fluid flow direction is defined and the synergy angle γ is investigated, as shown in Fig. 11. The synergy angle γ of the conical spiral tube bundle is larger than that of bare tube in the same condition. In another way, the field synergy between velocity gradient vector ∇u and the temperature gradient vector ∇T in the conical spiral tube bundle is better than that that in the bare tube. Therefore, comprehensive performance of conical spiral tube bundle is relatively improved.

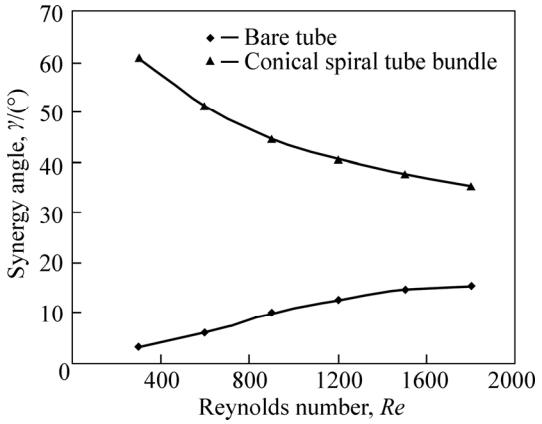

Fig. 11 Relationship between synergy angle γ and Reynolds number Re

5.3 Outer surface heat transfer

The heat transfer experiment of the planar elastic tube bundle was conducted under the constant heat flow condition [3]. The constant heat flow condition was achieved by the electric heating inside the elastic tube bundle, and the variation of the convective heat transfer coefficient outside the elastic tube bundle was investigated. In the experiment, the heat transfer

performances of elastic tube bundles were compared with those of the fixed bare tube in condition of same shell-side fluid flow speed. The heat transfer of the outer surface of planar elastic tube bundle is calculated with the formula by ZUKAUSKAS [25]:

$$Nu = CRe^{m}Pr^{1/3}(Pr/Pr_{w})^{0.25} \quad (10)$$

where C is a constant related to the fluid flow velocity, Nu is the Nusselt number, Re is the Reynolds number, the power exponent m is a constant, Pr is the Prandtl number of the outside fluid, and Pr_w is the Prandtl number of the outer surface of the tube bundle.

The correlation of outer surface heat transfer of the planar elastic tube bundle proposed by CHENG et al [3] is as follows:

$$Nu = 0.9Re^{0.6}Pr^{1/3}(Pr/Pr_{w})^{0.25} \quad (11)$$

The heat transfer of planar elastic tube bundle is compared with that of a fixed bare tube, and the experimental data indicate that the heat transfer coefficient of the elastic tube bundle is about 3 times that of the fixed bare tube in the same shell-side fluid flow velocity. The outer surface heat transfer of the improved planar elastic tube bundle mentioned above (seen in Fig. 12) is tested and the results indicate that the heat transfer of the improved tube bundle is increased by about 26% compared with the primary one [5].

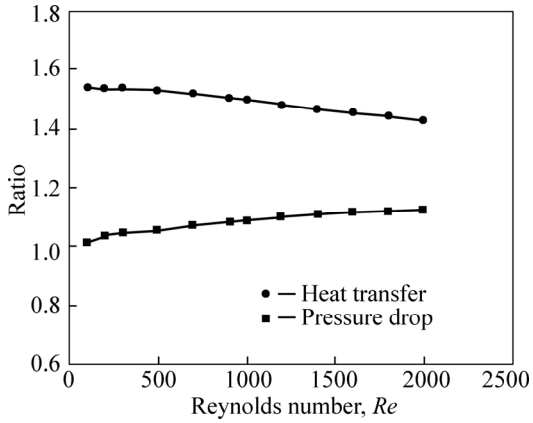

Fig. 12 Ratio of heat transfer and pressure drop of conical spiral tube bundle to planar elastic tube bundle

The further work done by SONG et al [6] proposed a novel installation structure of the planar elastic tube bundles. Two tube bundles were connected and an additional shell was approached to change the flow direction of the shell-side fluid flow in the heat exchangers, and the heat transfer coefficient was increased.

The research on the outer surface heat transfer of the conical spiral tube bundle was few due to the complex structure both in the simulation and experimental work. The fluid flow and the flow-induced vibration in the shell-side of conical spiral tube bundle heat exchangers were much different from those of planar elastic tube bundles, and the research work of this field is highly desirable.

6 Conclusions

1) The natural lower frequencies of planar elastic tube bundle are much larger than those of the conical spiral tube bundle. In condition of inside fluid flow, the critical fluid flow speed of planer elastic tube bundle is also higher than that of the conical spiral tube bundle.

2) The stress concentration takes place when the planar elastic tube bundle vibrates in the out-plane mode shape, while the stress distribution of the conical spiral tube bundle is uniform when the tube bundle vibrates in the longitudinal mode. The maximum stress of conical spiral tube bundle is only 1/5 that of the planar tube bundle in the same vibrating amplitude. Experimental data indicate that the stress and heat transfer of the novel planar tube bundle are greatly improved.

3) The secondary fluid flow inside the conical spiral tube is more intensive than that inside the planar elastic tube bundle, and the comprehensive performance of the conical spiral tube bundle is about 1.5 times that of the planar elastic tube bundle.

4) The shell-side heat transfer of the planer elastic tube bundle is about 3 times that of the fixed bare tube. The investigation on the heat transfer performance of the conical spiral tube bundle is highly desirable.

Nomenclatures

A	Cross section area of tube bundle
c	Flow velocity inside tube bundle
C	Constant related to flow velocity
$\boldsymbol{D}$	Dynamic matrix of system
f_0	Resistance coefficient of a bare tube
f_1	Resistance coefficient of planar elastic tube bundle
f_2	Resistance coefficient of conical spiral tube bundle
F	Symmetrical force
$\boldsymbol{G}$	General damp matrix
$\boldsymbol{K}_p$	General stiffness matrix
$\boldsymbol{K}_f$	Fluid kinetic matrix
m	Constant of power exponent
$\boldsymbol{M}$	General mass matrix
M_{max}	Maximum moment
n	Number of finite elements of tube bundle
Nu_0	Nusselt number of a bare tube
Nu_1	Nusselt number of planar elastic tube bundle
Nu_2	Nusselt number of conical spiral tube bundle

Pr Prandtl number of fluid
Pr_w Prandtl number of tube surface
q Node displacement of tube bundle
R Pipe curving radius
Re Reynolds number
U Distortion energy
w_z Bending section modulus
λ Eigenvalue
$\boldsymbol{\varphi}$ Vector of eigenvalue
δ_y Deflection of tube
Θ Cross section rotation angle
σ_{max} Maximum tensile stress
γ Synergy angle
∇T Temperature gradient vector
∇u Velocity gradient vector

References

[1] WEAVER D S, FITZPATRICK J A. A review of cross-flow induced vibration in heat exchanger tube arrays [J] Journal of Fluids and Structures, 1988, 2: 73−93.

[2] PETTIGREW M J, TAYLOR C E. Two-phase flow-induced vibration: An overview [J] Journal of Pressure Vessel Technology, 1994, 116(3): 233−253.

[3] CHENG Lin, LUAN T, DU W, XU M. Heat transfer enhancement by flow-induced vibration in heat exchangers [J] International Journal of Heat and Mass Transfer, 2009, 52(3): 1053−1057.

[4] CHENG Lin. Principle and application of elastic tube heat exchanger [M]. Beijing: Science Publishing House, 2001: 21−30. (in Chinese)

[5] JIANG Bo. Analysis on mechanism of heat transfer enhancement by vibration and experimental research on a new type of heat transfer component [D]. Jinan, China: Shandong University, 2010. (in Chinese)

[6] SONG Cui-hua, LI Dan, SHANG Ji-quan. Development of a brand new regenerative heat exchanger [J]. Journal of Shandong Institute of Light Industry (Natural Science Edition), 2001, 15(2): 4−8. (in Chinese)

[7] YAN Ke, GE Pei-qi, BI Wen-bo, SU Yan-cai. Vibration characteristics of fluid structure interaction of conical spiral tube bundle [J]. Journal of Hydrodynamics, 2010, 22(1): 121−128.

[8] ZHENG Ji-zhou, CHENG Lin, DU Wen-jing. Dynamic characteristics of elastic tube bundles with component mode synthesis method [J]. Chinese Journal of Mechanical Engineering, 2007, 43(7): 202−206. (in Chinese)

[9] YAN Ke, GE Pei-qi, SU Yan-cai, BI Wen-bo. Mathematical analysis on transverse vibration of conical spiral tube bundle with external fluid flow [J]. Journal of Hydrodynamics, 2010, 22(6): 816−822.

[10] YAN Ke, GE Pei-qi, ZHANG Lei, BI Wen-bo. Study on vibration characteristics of planar elastic tube bundles conveying fluid with finite element method [J]. Chinese Journal of Mechanical Engineering, 2010, 46(18): 145−149. (in Chinese)

[11] NI Zhen-hua, TIAN Jie. Dynamics analysis of spiral tube system conveying fluid by substructure synthesis [J]. Chinese Journal of Applied Mechanics, 1996, 13(3): 138−143. (in Chinese)

[12] NI Zhen-hua, ZHANG Huan. Vibration analysis of spiral tubes conveying fluid by finite element method [J]. Computational Structural Mechanics and Applications, 1992, 9(5): 153−162. (in Chinese)

[13] XU Zhi-xin, CHEN Yu-yue. Analysis of dynamic response of conveying fluid [J]. Shanghai Mechanics, 1983, 1: 1−11. (in Chinese)

[14] FU Yong-hua. Basic of finite element method [M]. Wuhan: Publishing House of Wuhan University, 2003: 79−81. (in Chinese).

[15] GUILMINEAU E, QUEUTEY P. A numerical simulation of vortex shedding from an oscillating circular cylinder [J]. Journal of Fluids and Structures, 2002, 16(6): 773−794.

[16] GOPALKRISHNAN R. Vortex induced forces on oscillating bluff cylinders [D]. Cambridge, MA, USA, Department of Ocean Engineering, MIT, 1993.

[17] SARPKAYA T. A critical review of the intrinsic nature of vortex-induced vibrations [J]. Journal of Fluids and Structures, 2004, 19: 389−447.

[18] ZHENG Ji-zhou. Dynamic characteristics of components of elastic tube bundle heat exchanger [D]. Jinan, China: Shandong University, 2007. (in Chinese)

[19] PAN Zhi-yuan, CUI Wei-cheng, LIU Ying-zhong. Prediction model for vortex-induced vibration of circular cylinder with data of forced vibration [J]. China Ocean Engineering, 2007, 21(2): 239−254.

[20] MENG Ji-an, CHEN Ze-jing. Experimental and numerical study on heat transfer and flow resistance in alternating elliptical axis tubes [J]. Journal of Engineering Thermophysics, 25(5): 813−815.

[21] YAN Ke, GE Pei-qi, SU Yan-cai, MENG Hai-tao. Numerical simulation on heat transfer characteristic of conical spiral tube bundle [J]. Applied Thermal Engineering, 2011, 31: 284−292.

[22] GUO Z Y, LI D Y, WANG B X. A novel concept for convective heat transfer enhancement [J]. International Journal of Heat and Mass Transfer, 1998, 41(14): 2221−2225.

[23] TAO W Y, GUO Z Y, WANG B X. Flied synergy principle for enhancing convective heat transfer-its extension and numerical verification [J]. International Journal of Heat and Mass Transfer, 2002, 45: 3849−3856.

[24] LIU W, LIU Z C, GUO Z Y. Physical quantity synergy in laminar flow field of convective heat transfer and analysis of heat transfer enhancement [J]. Chinese Science Bulletin, 2009, 54: 3579−3586.

[25] ZUKAUSKAS A. Heat transfer from tubes in crossflow [J]. Advances in Heat Transfer, 1972, 8: 93−160.

(Edited by YANG Bing)